Monte Carlo study of kink effect in isolated-gate InAs/AlSb High Electron Mobility Transistors

B. G. Vasallo[*1], H. Rodilla[1], T. González[1], G. Moschetti[2], J. Grahn[2], and J. Mateos[1]

[1]Depto. de Física Aplicada, Universidad de Salamanca,

Plaza de la Merced s/n, 37008 Salamanca, Spain

Phone: +34 923294436 Fax: +34 923294584 [*] E-mail: bgvasallo@usal.es

[2]Microwave Electronics Laboratory, Dept. of Microtechnology and Nanoscience,

Chalmers, University of technology, Göteborg, Sweden

ABSTRACT

A semiclassical 2D ensemble Monte Carlo simulator is used to perform a physical microscopic analysis of kink effect in InAs/AlSb High Electron Mobility Transistors (HEMTs). Due to the small bandgap of InAs, these devices are very susceptible to suffer impact ionization processes, with the subsequent hole transport through the structure, both implicated in the kink effect. The results indicate that, for high enough V_{DS}, holes generated by impact ionization tend to pile up in the buffer (at the gate-drain side) due to the valence-band energy barrier between the buffer and the channel. Due to this accumulation of positive charge the channel is further opened and I_D increases, leading to the kink effect in the *I*-*V* characteristics and even to the device breakdown. The microscopic understanding of this phenomenon provides useful information for a design optimization of kink-effect-free InAs HEMTs.

I. INTRODUCTION

Sb-based heterostructures, based on narrow band-gap semiconductors, in particular AlSb/InAs, are being considered to further improve the performance of High Electron Mobility Transistors (HEMTs) for low-power, high-frequency and low-noise applications.[1-5] However, these devices present some problems to be eliminated, as the kink effect, caused by impact ionization and the subsequent hole dynamics in the structure. In order to decrease the associated excessive gate leakage current, the conventional Schottky contact has been replaced by an insulated gate (by means of a native oxide, which naturally appears after the recess etch step[6]). However, impact ionization is still significant, and a study of the involved physical effects is important to further optimize the structure design and thus eliminate the negative consequences of kink effect.

The aim of this work is to perform a microscopic analysis of kink effect in recessed isolated-gate AlSb/InAs HEMTs. To this end, carriers dynamics in these devices is monitored by means of a semi-classical 2D ensemble Monte Carlo (MC) simulator[7,8] adequately adapted to correctly model AlSb/InAs heterostructures[9], in which both impact ionization and hole transport are included[10,11]. MC method has been proved to be a very useful tool when dealing with problems where the understanding of the microscopic behavior of carriers is essential, as occurs when analyzing kink effect phenomena[10,11]. Besides, the MC technique becomes the most adequate simulation tool since electron transport can easily turn into ballistic or at least quasiballistic in the channel of the analyzed transistors, because of the very high mobility of InAs[9]. This approach allows to determine the origin and magnitude of the kink effect in terms of internal quantities, like electron and hole concentrations and electric field profile, so that a complete physical understanding of the kink phenomenon in these devices is achieved, thus providing helpful information for the development of Sb-HEMTs with improved immunity to this effect.

The paper is organized as follows. In Sec. II the physical model is detailed. The main results of our simulations and their discussion are provided in Sec. III. Finally, in Sec. IV we draw the most important conclusions of this work.

II. PHYSICAL MODEL

For the calculations we make use of an ensemble MC simulator self-consistently coupled with a 2D Poisson solver which incorporates all the processes at the origin of the kink effect. The simulated structure is very similar to the experimental one described in Ref. [5], what will be used to calibrate our model by reproducing the static characteristics. The structure under analysis is a 225 nm T-gate recessed HEMT [Fig. 1(a)], fabricated on a heterostructure consisting of a InP substrate (not simulated), a 800 nm AlSb buffer followed by a 15 nm thick InAs channel, two layers of AlSb (a 5 nm spacer and a 10 nm Schottky layer, separated by a 5×10^{12} cm^{-2} δ-doped layer), and, finally, a 4 nm thick AlInAs and 5 nm thick InAs cap layer (N_D= 5×10^{18} cm^{-3}). The MC parameters for the electron transport simulation in the involved materials can be found in Ref. [9]. Fig. 1(b) presents the conduction and valence bands provided by the MC simulations for the AlSb/InAs heterostructure.

Impact ionization of electrons, which occurs in the Γ valley of InAs and leads to the appearance of holes, is included in the MC simulations by using the Keldysh approach,[12] where the probability per unit time of having an impact ionization event is given by $P(E) = S\left[(E-E_{th})/E_{th}\right]^2$ if $E > E_{th}$, and $P(E) = 0$ if $E < E_{th}$, E being the electron kinetic energy in the Γ valley, E_{th} the ionization threshold energy and S a measure of the softness or hardness of the threshold. E_{th} and S are considered as adjustable parameters to reproduce the ionization coefficient (number of impact ionization events that occur per unit length) measured in bulk materials. From each impact ionization occurrence, an electron in the Γ valley and a hole in the heavy-hole band emerge, while the electron originating the ionization process remains in the Γ valley. We have verified that hole impact ionization is negligible for the considered applied voltages. Fig. 2 presents, for InAs (channel material), the simulated values of (a) the electron velocity with and without considering impact ionization in the simulations as a function of the electric field, and (b) the impact ionization coefficient for E_{th}=0.41 eV and $S = 10^{12}$ s^{-1} as a function of the inverse of the electric field in comparison with the results obtained in Refs. [12] and [13]. For these values of E_{th} and S, a remarkable agreement in the impact ionization curves is achieved. According to Fig. 2(a), when impact ionization is considered, the electron peak velocity is higher than in the case of neglecting impact ionization processes. This occurs because the onset of impact ionization takes place for electron energies lower than those necessary for

intervalley transfer (otherwise very frequent in bulk InAs), so that the electron occupancy in the Γ valley is higher than in the case of absence of impact ionization. As a consequence, the maximum electron velocity increases and takes place for a higher electric field.[9]

With respect to the model used for hole dynamics, a typical spherical and nonparabolic valence band structure is considered, including three sub-bands: heavy- and light-hole bands (HH and LH), degenerated at $\mathbf{k}=0$ and characterized by a different curvature in $\mathbf{k}$-space, and a third split-off band (SOH), in which the band warping is accounted for by the use of approximated overlap functions.[14] Ionized impurity, acoustic, polar and non-polar optical phonon scattering mechanisms are considered for holes.[14,15] The hole physical parameters used in the simulations are reported in Table I, providing a low-electric-field mobility of 350 cm^2/Vs.

Another important process that is necessary to take into account for a proper analysis of kink effect is hole recombination.[10] To this end we use a simple model in which hole recombination is considered to take place with a characteristic time τ_{rec} (i.e., with a probability $1/\tau_{rec}$). We will perform simulations with τ_{rec}=0.5 ns (even if in bulk materials it is usually considered to be of the order of 1 ns), since with this value of τ_{rec} (jointly with those of E_{th} and S) the experimental static I-V characteristics are adequately reproduced, as we will show in Sec. III.

III. RESULTS

Fig. 3 shows the simulated (a) extrinsic and (b) intrinsic output characteristics of the InAs-HEMT in presence and absence of impact ionization. The experimental I-V curves taken from [5] have been included in Fig. 3(a) for comparison. In order to carry out the comparison of the measured results (extrinsic) with those obtained from the simulation (intrinsic), it is necessary to include, in a postprocessing stage, the parasitic elements that are not considered in the intrinsic MC model.[16] Thus, drain and source parasitic resistances associated with metallizations and part of the ohmic regions not included in the simulation domain have been incorporated into the original MC results, with the best fit being obtained for R_S=0.13 Ω·mm and R_D=0.38 Ω·mm. A remarkable agreement between experimental and simulated results is reached when considering impact ionization in the simulations with values for the involved parameters of E_{th}=0.41 eV, $S=10^{12}$ s^{-1} and τ_{rec}=0.5 ns, as mentioned previously. A notable increase of I_D takes place starting from a value of V_{DS} high

enough for the onset of impact ionization. In the inset of Fig. 3(b), the difference in the values of I_D obtained with and without considering impact ionization is plotted as a function of V_{GS} for different values of V_{DS}. The increase of I_D for a fixed V_{DS} due to the appearance of holes grows with V_{GS}. This behavior is the opposite of that found for lattice-matched InGaAs/InAlAs HEMTs, in which the increase of I_D is lower for higher V_{GS}, which occurs because although the electron concentration in the channel is larger when the channel opens, the maximum electron energy is reduced due to the lower gate-to-drain potential.[10,11] In the case of InAs/AlSb HEMTs, the GAP of the channel material is much smaller, and then the threshold energy E_{th}, thus impact ionization probability still remains significant for higher values of V_{GS}. Besides, impact ionization events take place not only near the maximum of electron energy (under the gate electrode), but all along the drain-side of the channel, where the electron velocity is higher when increasing V_{GS}, as will be shown later.

The isolated gate allows reducing the gate leakage current, but it still shows the typical bell-shape due to the outflow of holes, signature of impact ionization in standard Schottky-Gate FETs[6]. I_G is null in the ideal simulated structures, since the gate current due to hole tunneling is not considered in our model.

MC simulations provide an insight into the microscopic processes taking place inside the devices, in terms of which the kink effect can be explained. Initially, the influence of V_{GS} will be analyzed. Fig. 4 shows the profiles along the channel of: (a) the number of impact ionization events taking place in the channel, (b) the sheet hole density in the buffer and the cap layer, (c) the sheet electron density, and (d) mean electron velocity in the channel, for V_{DS}=0.4 V and different values of V_{GS}. As observed in Fig. 4(a), the impact ionization events take place in the drain side of the channel, mainly close to the drain side of the recess, where the electric field, and consequently the electron energy, is higher. In fact, kink effect is commonly avoided (actually shifted to higher biasings) by enlarging the drain recess length, which leads to a lower electric field in that region. Moreover, the few impact ionization events taking place in the InAs cap layer lead to a concentration of holes moving towards the gate electrode and piling up in the gate side of the cap layer [Fig. 4(b)], where they disappear by recombination.

Most of the holes generated by impact ionization in the channel descend the energy step present in the valence band at the heterojunction between the InAs channel and the AlSb buffer [Fig. 1(b)]. Once the holes energy decreases because of scattering mechanisms, the attracting force of the gate potential and the negative surface charge at the recess is

not sufficiently strong for them to surmount back the energy barrier in the valence band. Thus they accumulate in the buffer, mainly at the drain side [Fig. 4(b)]. The increase of I_D can be mostly explained as a consequence of this pile up of positive charge, which lowers the potential barrier that controls the current through the channel, so that the channel is further opened, with the consequent increase in the electron density [Fig. 4(c)] and drain current. The rise of I_D is basically due to this enhancement in the electron flow through the channel, since the number of electrons/holes generated by impact ionization is very low so as to provide a significant contribution to I_D. As well, the mean value of the electron velocity [Fig. 4(d)] is higher at the drain side of the channel for higher values of V_{GS}, which contributes also to the enhancement of I_D. Notice than both electron concentration and mean velocity are higher at the drain side of the channel for increasing values of V_{GS} while at the source side the electron density is similar, which leads to larger differences in the mean velocity. Few holes reach the source contact because, as explained before, they tend to pile up in the buffer at the drain side and under the gate, and recombine before reaching the source.

The effect of this pile-up of holes in the buffer can be observed in the behavior of the vertical electric field. In Fig. 5 the vertical electric field under the source-side of the recess is represented along the vertical direction in both simulated cases, with and without considering impact ionization, for a bias of V_{DS}=0.4 V and V_{GS}=-0.6 V. When the hole accumulation is not present in the structure, the electric field in the channel takes positive values; then, electrons tend to move up and flow through the upper side of the channel. However, the presence of the hole pile-up originates a negative vertical electric field near the buffer, which leads to a higher quantity of electrons entering into the active part of the device, many of them flowing through the bottom side of the channel.

To further illustrate this effect, Fig. 6 presents the contour maps of (a) the difference between the electron density with and without considering impact ionization, and (b) hole density, for a bias of V_{DS}=0.4 V and V_{GS}=-0.6 V. Since the hole pile-up takes place in the buffer, the difference in electron density under the gate between the two cases is higher at the bottom side of the channel than at the top side. However, the most important increase of electron concentration appears at the drain side of the channel, thus further increasing the drain conductance of the transistor, and the kink observed in the *I-V* curves.

IV. CONCLUSIONS

We have presented a microscopic analysis of kink effect in insulated-gate recessed AlSb/InAs HEMTs based on MC simulations. The results allow interpreting the effect in terms of the pile up of holes (generated by impact ionization at the drain region of the channel) at the drain-gate side of the buffer. This hole pile-up takes place in the buffer because of the energy barrier in the valence band at the heterostructure between the AlSb buffer and the InAs channel. The positive charge due to the accumulation of holes contributes to further open the channel below the gate, mainly through its bottom side thus increasing the electron density in the active part of the device. Moreover, impact ionization produces an important enhancement of the electron concentration at the drain side of the channel, leading to a further increase of the drain conductance and the kink effect in the *I-V* curves.

ACKNOWLEDGMENTS

This work has been partially supported by the European Commission through the ROOTHz Project ICT-2009-243845 and the MC2ACCESS Project, by the Dirección General de Investigación (MEC) and FEDER through Project TEC2007-61259/MIC and by the Consejería de Educación, Junta de Castilla y León through Project SA019A08.

REFERENCES

[1] C. R. Bolognesi, M. W. Dvorak, and D. H. Chow, IEEE Trans. Electron Devices **46**, 826 (1999).

[2] J. B. Hacker, J. Bergman, G. Nagy, G. Sullivan, C. Kadow, H.-K. Lin, A., C. Gossard, M. Rodwell, and B. Brar, IEEE MTT-S Int. Microwave Symp. Dig. 2005, 1029.

[3] W. Kruppa, J. B. Boos, B. R. Bennett, N. A. Papanicolaou, D. Park, and Robert Bass, IEEE Trans. Electron Devices **54**, 1193 (2007).

[4] Y. C. Chou, M. D. Lange, B. R. Brennett, J. B. Boos, J. M. Yang, N. A. Papanicolau, and C. H. Lim, IEEE Electron Device Lett. **28**, 856 (2007).

[5] M. Malmkvist, E. Lefebvre, M. Borg, L. Desplanque, X. Wallart, G. Dambrine, S. Bollaert, and J. Grahn, IEEE Trans. Microwave Theory Tech. **56**, 2685 (2008).

[6] E. Lefebvre, M. Malmkvist, M. Borg, L. Desplanque, X. Wallar, G. Dambrine, S. Bollaert, and J. Grahn, IEEE Trans. Electron Devices **56**, 1904 (2009).

[7] J. Mateos, T. González, D. Pardo, V. Hoel, H. Happy, and A. Cappy, IEEE Trans. Electron Devices **47**, 250 (2000).

[8] J. Mateos, T. González, D. Pardo, V. Hoel, and A. Cappy, Semicond. Sci Technol **14** 864 (1999).

[9] H. Rodilla, T. González, D. Pardo, and J. Mateos, J. Appl. Phys. **105**, 113705 (2009).

[10] B. G. Vasallo, J. Mateos, D. Pardo, and T. González, J. Appl. Phys. **94**, 4096 (2003).

[11] B. G. Vasallo, J. Mateos, D. Pardo, and T. González, J. Appl. Phys. 95, 8271 (2004).

[12] M. V. Fischetti, IEEE Trans. Electron Devices 38, 634 (1991).

[13] K. Brennan, and K. Hess, Solid-State Electron. 27, 347 (1984).

[14] T. Brudevoll, T. A. Fjeldly, J. Baek, and M. S. Shur, J. Appl. Phys. **67**, 7373 (1990).

[15] M. Costato, and L. Reggiani, Phys. Stat. Sol. (b) **58**, 471 (1973).

[16] S. Babiker, A. Asenov, N. Cameron, and S. P. Beaumont, IEEE Trans. Electron Devices **43**, 2032 (1996).

FIGURE CAPTIONS

TABLE 1. Physical parameters of holes in InAs and AlSb.

FIG. 1. (a) Schematic drawing of the HEMT topology used in the simulations. (b) Conduction and valence bands for the AlSb/InAs heterostructure under analysis.

FIG. 2. MC values in bulk InAs of (a) the electron velocity in both cases with and without considering impact ionization vs. electric field and (b) impact ionization coefficient vs. inverse of electric field in comparison with the values in Refs. [12] and [13]. $E_{th} = 0.41\,\mathrm{eV}$, $S = 10^{12}\ \mathrm{s}^{-1}$.

FIG. 3. MC (a) extrinsic and (b) intrinsic output characteristics for the InAs/AlSb HEMT in presence and absence of impact ionization, being $E_{th} = 0.41\,\mathrm{eV}$, $S = 10^{12}$ s^{-1} and τ_{rec}=0.5 ns. Experimental results of the similar fabricated structure are plotted in (a) for comparison. V_{GS} is -0.40 V for the top curves and the potential step is ΔV_{GS}=-0.1 V. Inset: difference of I_D with and without considering impact ionization vs. V_{GS} for different V_{DS}.

FIG. 4. Profiles along the channel of: (a) impact ionization events in the channel per unit time and depth, (b) hole sheet density in the buffer and the cap layer, (c) sheet electron density, and (d) mean electron velocity in the channel for different values of V_{GS}, being V_{DS}=0.4 V, $E_{th} = 0.41$ eV, $S = 10^{12}\,\mathrm{s}^{-1}$ and τ_{rec}=0.5 ns. The position of the gate and the recess is also indicated.

FIG. 5. Vertical electric field profile along the X-direction under the source side of the recess in presence and absence of impact ionization for V_{DS}=0.4 V, V_{GS}=-0.6 V, $E_{th} = 0.41$ eV, $S = 10^{12}\,\mathrm{s}^{-1}$ and τ_{rec}=0.5 ns. The position of the different active layers is also indicated.

FIG. 6. Contour maps of (a) the difference between the electron density with and without considering impact ionization, and (b) hole density, for V_{DS}=0.4 V, V_{GS}=-0.6 V, $E_{th} = 0.41$ eV, $S = 10^{12}\,\mathrm{s}^{-1}$ and τ_{rec}=0.5 ns. The position of the gate and the recess is also indicated.

PARAMETER	InAs			AlSb		
GAP (eV)	0.354			1.615		
Optical phonon energy (eV)	0.03			0.036		
Optical deformation potential (eV / m)	11.3			11.3		
Acoustic deformation potential (eV)	20.0			6.64		
	HH	LH	SOH	HH	LH	SOH
Effective mass (m^* / m_0)	0.570	0.025	0.140	0.6035	0.1070	0.2200
Nonparabolicity (1/eV)	1.0	0.9	0.8	1.0	0.9	0.8
Energy level from HH (eV)	0.0	0.0	0.39	0.0	0.0	0.973

Table 1

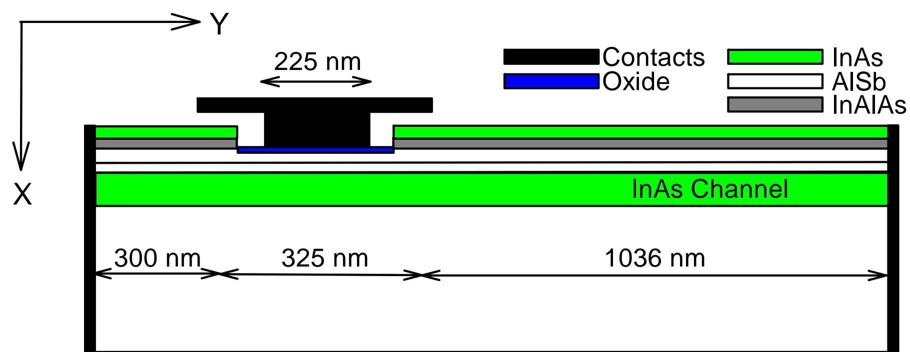

(a)

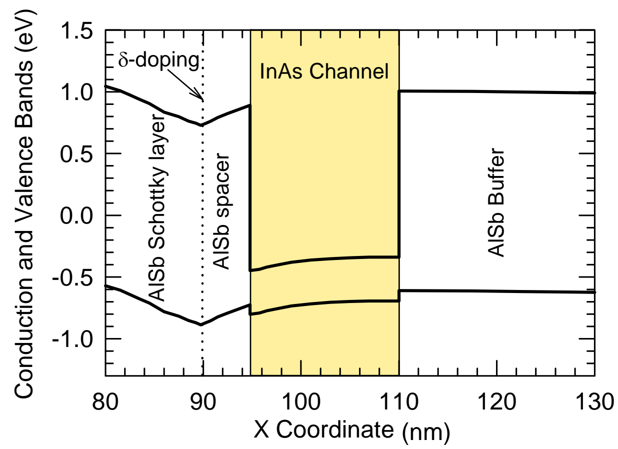

(b)

FIG. 1

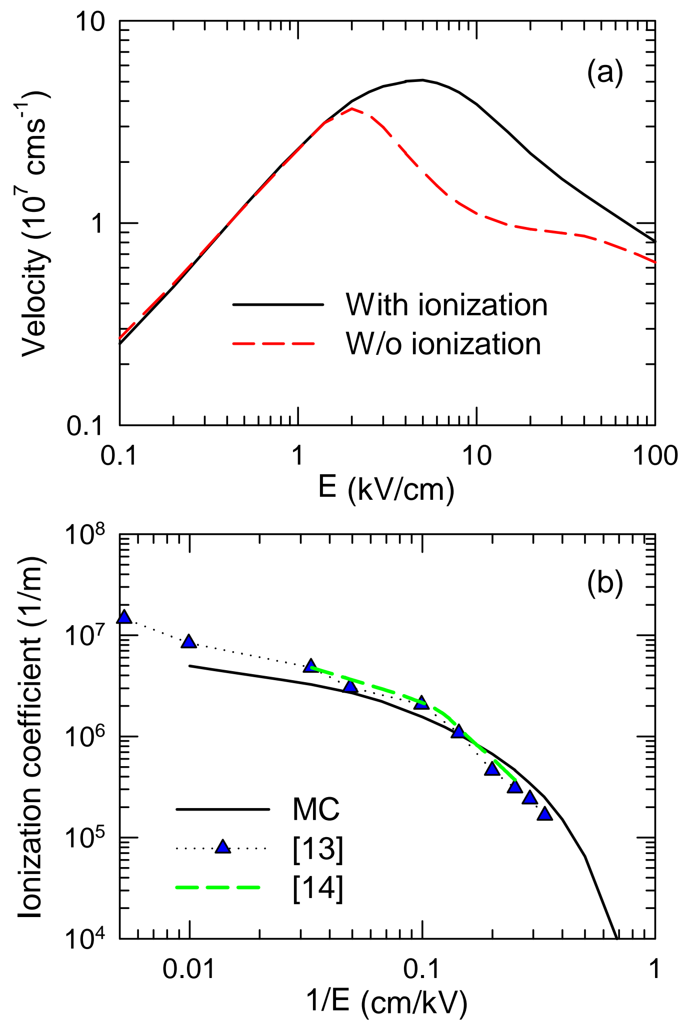

FIG. 2

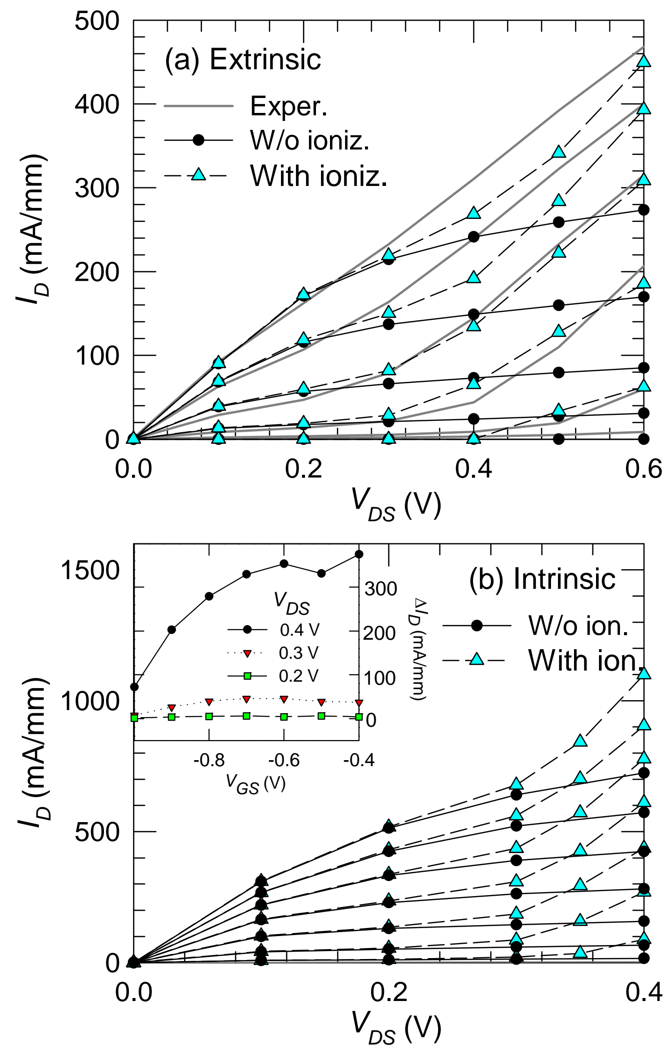

FIG. 3

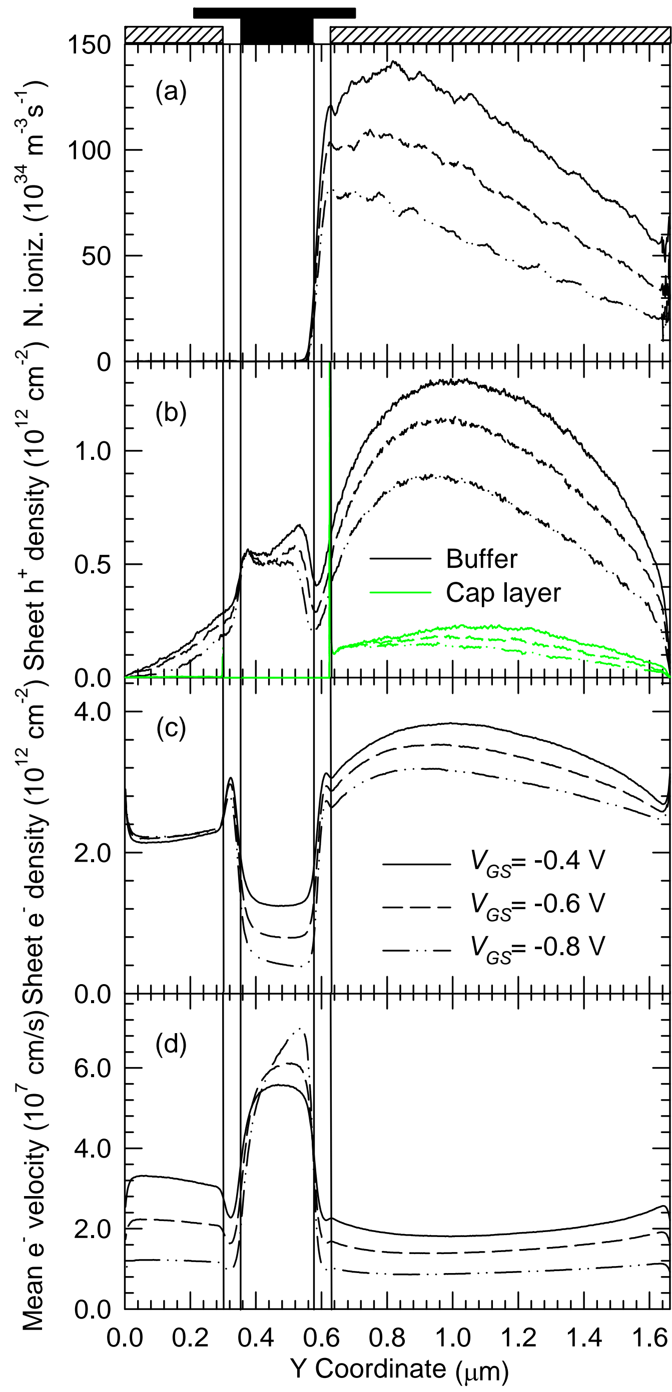

FIG. 4

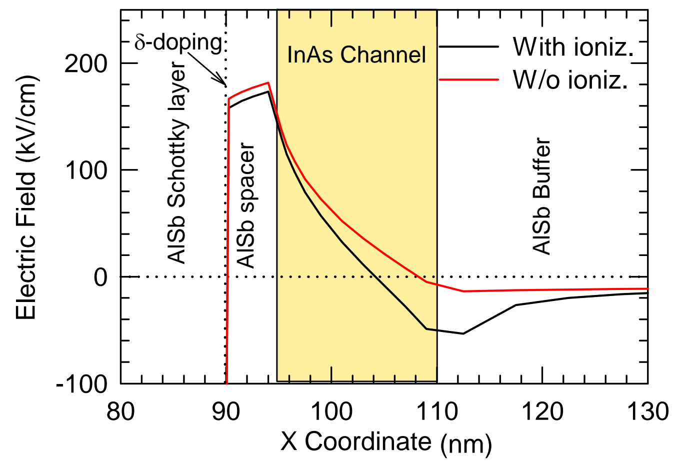

FIG. 5

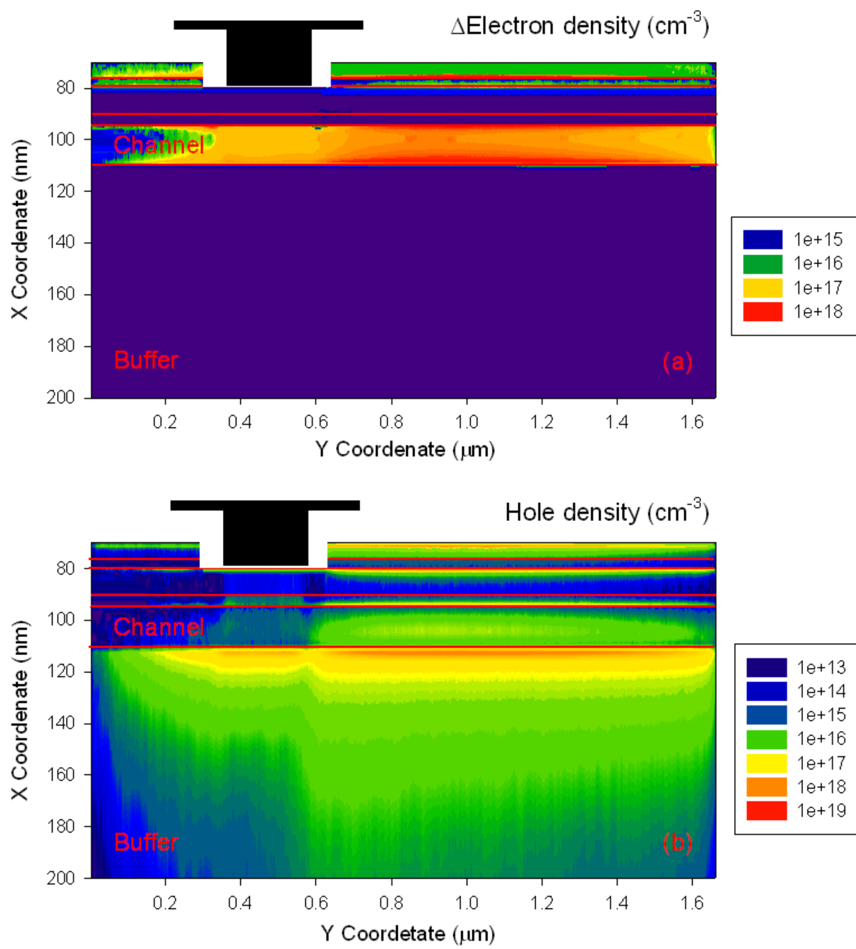

FIG. 6